result in a prohibitively high activation energy. Rotamer *E*-**5** may be excluded because of its high ground-state energy. Of the remaining *E* conformers only *E*-**2** has the desired proximity of the basic nitrogen lone pair to the incipient hydrogen that is to be transferred in the transition state, **15**, for epoxidation. Significantly, this conformer will be highly populated as a result of its inherent stability. We therefore suggest that the syn *E* conformer **2** is the effective oxidizing agent in oxirane formation with an alkene.

By analogy to our previous theoretical study on the mechanism of epoxidation of alkenes with peroxyformic acid (**1**),[10a] we invoke a backside displacement by the carbon–carbon π-bond (HOMO) on the empty σ^* orbital of the peroxide bond with the orientation depicted in **13**. The transition state **15** may be achieved by O–O bond cleavage, and simultaneous conversion of the initial carbon–oxygen single bond into the carbonyl group of the product formamide by rotation about an axis through the formimide carbon atom and perpendicular to the imine plane (see **14**). The process is accompanied by a concomitant 1,4-hydrogen shift (**16**) which is necessary to effect a net bonding interaction between the terminal oxygen and the alkene carbon.

In conclusion, the overall epoxidation reaction can best be achieved by interaction of *E*-**2** with an alkene as suggested in Figure 12. The above conformational study indicates that this desired conformer is readily attainable and represents a large fraction of the equilibrium mixture of peroxyformimidic acid rotamers.

Acknowledgment. We gratefully acknowledge support from the National Institutes of Health (2 R01 ES00761-08A1) and the National Science Foundation (CHE-80-06520). The authors also wish to thank Professor Morton Raban for helpful discussions concerning the mechanism of imine isomerization and Dr. Frank Westervelt for generous amounts of computer time.

Principal Components of the Cadmium-113 Shielding Tensors in Cadmium Sulfate Hydrates: Nuclear Magnetic Resonance Study of Cadmium Coordinated with Oxygen

P. DuBois Murphy and B. C. Gerstein*

Contribution from Ames Laboratory,† Department of Energy, and Iowa State University, Ames, Iowa 50011. *Received August 22, 1980*

Abstract: A study is reported of the principal components of the ^{113}Cd NMR shielding tensors in the salts $3CdSO_4 \cdot 8H_2O$ and $CdSO_4 \cdot H_2O$. A discussion of the sensitivity of the principal components of the ^{113}Cd shielding tensors to coordination of the cadmium with nearest-neighbor oxygens is presented. An apparent anomaly between the observed shielding anisotropies and the proposed Cd–O bonding distances for $3CdSO_4 \cdot 8H_2O$ has prompted a refinement of the original crystal structure proposed by Lipson. The refined Cd–O bonding distances are found to be more uniform than those originally reported, in agreement with information inferred from the observed ^{113}Cd NMR shielding anisotropies.

Introduction

Solid-state, high-resolution NMR[1] provides a simple, yet powerful means for structural studies. Cheung et al.[2] have recently noted that ^{113}Cd shieldings are particularly sensitive to coordination with oxygen. Their studies showed a ^{113}Cd shielding dispersion of almost 300 ppm among the hydrated salts $2CdCl_2 \cdot 5H_2O$, $Cd(OH)_2 \cdot H_2O$, $3CdSO_4 \cdot 8H_2O$, $Cd(OAc) \cdot 2H_2O$, and $Cd(NO_3)_2 \cdot 4H_2O$. They also noted the two magnetically inequivalent ^{113}Cd species in the salt $3CdSO_4 \cdot 8H_2O$. Although Cheung et al. were not able to resolve the principal components of the two shielding tensors, they did observe that the apparent anisotropies of these tensors were the smallest of those studied.[2]

The purpose of the present work is to measure the principal components of the ^{113}Cd shielding tensors in the hydrated cadmium salts $3CdSO_4 \cdot 8H_2O$ and $CdSO_4 \cdot H_2O$. A comparison is made between the shielding parameters of Cd(II) in $3CdSO_4 \cdot 8H_2O$ and those[2] of the Cd(II) in $Cd(NO_3) \cdot 4H_2O$ for which the crystal structure is believed accurate. In particular, we note an incompatibility between the NMR data and Lipson's proposed crystal structure for $3CdSO_4 \cdot 8H_2O$: the observed ^{113}Cd shielding anisotropies do not appear consistent with the large variation in Cd–O bonding distances proposed by Lipson.[3] This observation has prompted a refinement, discussed below, of the crystal structure of $3CdSO_4 \cdot 8H_2O$.

Experimental Section

Instrumentation. ^{113}Cd-^1H cross polarization (CP) NMR measurements were performed at frequencies of 12.42 and 56.02 MHz for ^{113}Cd and ^1H in our 1.3-T laboratory field. The spectrometer was designed in our laboratory and is described in detail elsewhere.[2] The CP contact time was $t_{CP} = 4$ ms, rotating-frame H_1 fields were 8 and 36 G, and the time between scans was 3 s for $3CdSO_4 \cdot 8H_2O$ and 9 s for $CdSO_4 \cdot H_2O$. Both magic-angle-spinning (MAS)[1] and off magic-angle-spinning (OMAS)[4,5] experiments were performed with rotor speeds of 2.5 kHz. Static measurements resulted from 8000/15 000 signal averages; MAS and OMAS, 500/800. The low-frequency filter bandwidths were 2 and 10 kHz for the MAS/OMAS and static measurements, respectively. Chemical shifts are reported with respect to an external standard of $Cd(NO_3)_2 \cdot 4H_2O$, and negative shifts are downfield (decreased shielding). Because of the possibility of bulk susceptibility errors,[6] shieldings are believed accurate to ±5 ppm. All measurements were made at room temperature.

Preparation of Samples. Hydrate samples were prepared from reagent-grade $3CdSO_4 \cdot 8H_2O$ crystals (Fisher No. 72089). In fact, quantitative analysis showed this reagent to be 47.0 ± 2% Cd and 15.5 ± 0.1%

† Operated for the U.S. Department of Energy by Iowa State University under Contract No. W-7405-Eng-82. This research was supported by the Assistant Secretary for Energy Research, Office of Energy Sciences, WPAS-KC-03-02-01.

(1) Mehring, M. "High Resolution NMR Spectroscopy in Solids"; Springer-Verlag: Berlin, 1976.
(2) Cheung, T. T. P.; Worthington, L. E.; Murphy, P. DuBois; Gerstein, B. C. *J. Magn. Reson.* **1980**, *41*, 158.
(3) Lipson, H. *Proc. R. Soc. London, Ser. A* **1936**, *156*, 462.
(4) Stejskal, E. O.; Schaefer, J.; McKay, R. A. *J. Magn. Reson.* **1977**, *25*, 569.
(5) Taylor, R. E.; Pembleton, R. G.; Ryan, L. M.; Gerstein, B. C. *J. Chem. Phys.* **1979**, *71*, 4541.
(6) Pople, J. A.; Schneider, W. G.; Berstein, H. J. "High-Resolution Nuclear Magnetic Resonance"; McGraw-Hill: New York, 1959.

0002-7863/81/1503-3282$01.25/0

Table I. ^{113}-Cd NMR Shielding Parameters for $3CdSO_4 \cdot 8H_2O$

conditions	^{113}Cd type	$\Delta\sigma'$ [a] ± 1 ppm	$\sigma_\parallel$ [b] ± 2 ppm	$\sigma_\perp$ ± 2 ppm	$\bar{\sigma}$ ± 2 ppm	$\Delta\sigma$ [c] ± 4 ppm	% area ± 2 %	fwhm [d] ± 0.5 ppm	R [e] ± 20 Hz
static	A		−101.4	−14.9	−43.7	−86.4	33.2	15.0	717
	B		−128.9	−20.8	−56.8	−108.0	66.8	15.0	895
OMAS	A	−2.9	−94.8	−17.8	−43.5	−77.0	32.3	1.2	637
$\theta = 53.2°$	B	−3.9	−124.6	−21.9	−56.1	−102.7	67.7	1.6	851
MAS	A				−43.7		35.1	0.7 [f]	
$\theta = 54.7°$	B				−56.2		64.9	0.8 [f]	
OMAS	A	5.3	−102.7	−14.1	−43.6	−88.6	34.5	1.6	734
$\theta = 57.2°$	B	6.5	−128.6	−20.3	−56.4	−108.3	65.5	1.8	897

[a] Scaled anisotropy measured only in OMAS experiment; static values calculated with eq 7 and 8 of text. [b] Shifts in ppm with respect to $Cd(NO_3)_2 \cdot 4H_2O$; negative shifts downfield; no bulk susceptibility corrections; accuracy with respect to external reference estimated to be ±5 ppm. [c] $\Delta\sigma = \sigma_\parallel - \sigma_\perp$; $\sigma_\parallel = \bar{\sigma} + 2\Delta\sigma/3$; $\sigma_\perp = \bar{\sigma} - \Delta\sigma/3$. [d] Full width at half-maximum of Gaussian broadening functions. [e] Rapid rotation criterion; $\omega_0 = 12.42$ MHz; see eq 6 of text. [f] Full width at half-maximum of absorption.

H_2O (mole ratio H_2O/Cd of 1.99/1, not 8/3). Examination of the "reagent" under a microscope revealed two crystalline materials: (1) a clear crystal which was identified as $3CdSO_4 \cdot 8H_2O$ by X-ray diffraction and (2) an opaque crystal which is believed to be $CdSO_4 \cdot H_2O$. Guinier X-ray measurements confirmed the presence of both hydrates in the "reagent".

NMR measurements were made on a freshly ground powder of $3CdSO_4 \cdot 8H_2O$ crystals. These crystals were prepared by slow evaporation of a solution of ca. 31 g of the reagent powder in 72 g of distilled H_2O. Large flat crystals formed in 3–5 days. Analysis of these crystals showed a mole ratio H_2O/Cd of 8.14/3. At room temperature, Duval[7] reports the phase $3CdSO_4 \cdot 8H_2O$ to be stable; at ca. 40 °C the salt begins to loose water, transforming itself into the monohydrate $CdSO_4 \cdot H_2O$ at 74 °C, which is stable to 156 °C. The sample of $CdSO_4 \cdot H_2O$, a fine white powder, was prepared by heating the $3CdSO_4 \cdot 8H_2O$ "reagent" at 105 °C for constant weight (approximately 4 h). Analysis of the monohydrate powder showed a mole ratio H_2O/Cd of 1.02/1. An "ultrapure" grade sample of CdS (Alfa) and an "analytical-grade" sample of CdO (Mallinckrodt) were used without further preparation. For these measurements, a phase-alternated single pulse experiment with MAS of 2.5 kHz was used. The period between accumulations was 30 s. All samples contained cadmium isotopes of natural abundance. Sample weights were ca. 0.4 g for all experiments.

Results and Discussion

Solid-state NMR studies of powders (referred to as static spectra) yield information about the principal components (σ_{11}, σ_{22}, and σ_{33}) of the diagonalized shielding tensor.[1] If two of the three shielding components are equal, the tensor is termed axially symmetric with $\sigma_\parallel = \sigma_{11}$ and $\sigma_\perp = \sigma_{22} = \sigma_{33}$. For a nonaxially symmetric shielding tensor with $\sigma_{11} < \sigma_{22} < \sigma_{33}$, the shielding anisotropy, $\Delta\sigma$, is defined:

$$\Delta\sigma = \sigma_{11} - (\sigma_{22} + \sigma_{33})/2 \quad (1)$$

For an axially symmetric tensor eq 1 reduces to

$$\Delta\sigma = \sigma_\parallel - \sigma_\perp \quad (2)$$

Magic-angle-spinning experiments directly measure the isotropic values, $\bar{\sigma}$, of these shielding tensors.[1] For a nonaxially symmetric tensor:

$$\bar{\sigma} = (\sigma_{11} + \sigma_{22} + \sigma_{33})/3 \quad (3)$$

and similarly for an axially symmetric tensor:

$$\bar{\sigma} = (\sigma_\parallel + 2\sigma_\perp)/3 \quad (4)$$

Static, OMAS and MAS spectra of $3CdSO_4 \cdot 8H_2O$ are shown in Figures 1 and 2. Appropriate spectral information is tabulated in Table I. The salt $3CdSO_4 \cdot 8H_2O$ contains two inequivalent ^{113}Cd species. The static powder pattern (top of Figure 1) results from the overlap of the powder patterns of their two shielding tensors. The MAS spectrum (middle) results from high-speed sample rotation[1] about an axis oriented at the magic angle of 54.7° to the static field. For such measurements shielding anisotropies vanish; the residual width of the lines is primarily determined by magnet inhomogeneity (about 0.5 ppm for our magnet) and slight offsets from the magic angle. The two inequivalent ^{113}Cd shieldings result in a severely overlapping static powder spectrum.

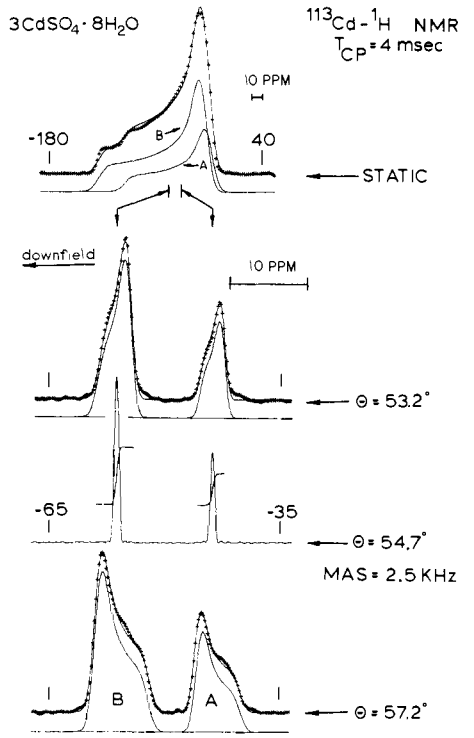

Figure 1. Solid-state ^{113}Cd NMR spectra of $3CdSO_4 \cdot 8H_2O$: (top) static powder pattern with superimposed shielding tensors directly below; (middle) magic angle spinning (MAS). Directly above and below the MAS spectrum are the off-magic-angle-spinning spectra (OMAS) which show resolved but scaled shielding tensors.

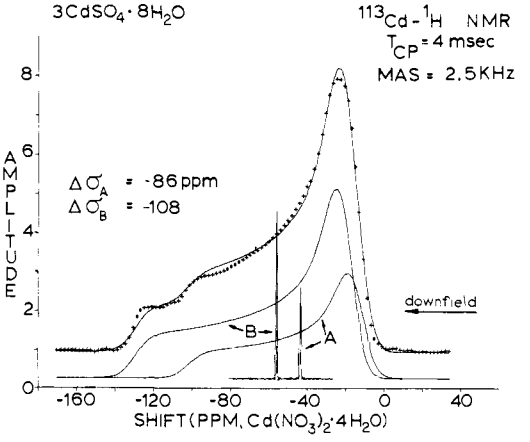

Figure 2. Solid-state spectrum of ^{113}Cd of $3CdSO_4 \cdot 8H_2O$ with superimposed axially symmetric shielding tensors (A and B) which contribute to the static powder pattern. Also shown is the MAS-narrowed spectrum.

(7) Duval, C. "Inorganic Thermogravimetric Analysis"; Elsevier: New York, 1963.

In order to measure their shielding parameters, an OMAS experiment[4,5] was performed.

The OMAS spectra result from spinning at small offsets from the magic angle and yield line shapes in which the shielding anisotropies are retained but scaled. To avoid the complexity of sidebands, rotation speeds, ω_r, must be in excess[5] of the rotation factor R. The conditions are:

$$\omega_r > R \tag{5}$$

$$R = \omega_0|\sigma_i - \bar{\sigma}| \tag{6}$$

where σ_i is chosen such that $|\sigma_i - \bar{\sigma}|$ is maximum. For example, the rotation factor for the $CdSO_4 \cdot H_2O$ tensor would be: $R = 12.42 \times |-139 - 47| = 1.14$ kHz based on the observed shielding components tabulated in Table II.

Knowledge of the rotation angle θ and the scaled shielding components, σ_i', allows one to calculate[5] the value of the static components, σ_i:

$$\sigma_i = (\sigma_i' - \bar{\sigma})/C + \bar{\sigma} \tag{7}$$

$$C = (3\cos^2\theta - 1)/2 \tag{8}$$

Anisotropies and isotropic values may then be calculated with eq 1–4. Note that the observed shielding anisotropies under OMAS invert for positive and negative offsets from the magic angle.

For example, the scale principal shielding components of the type A ^{113}Cd of $3CdSO_4 \cdot 8H_2O$ were measured as $\sigma_\parallel' = -45.4$ and $\sigma_\perp' = 42.5$ ppm at an off-magic-angle of 53.2°. The isotropic shift was recorded as $\bar{\sigma} = -43.5$ ppm at the magic angle of 54.7°. From eq 8, one calculates the scaling factor, $C = 3.82 \times 10^{-2}$. The inferred static principal components are then calculated by eq 7 as $\sigma_\parallel = -93.2$ and $\sigma_\perp = -17.4$ ppm. These inferred values are refined by subsequent least-squares analysis. Inferred static shielding anisotropies, $\Delta\sigma$, can be calculated directly from the scaled values, $\Delta\sigma'$, by dividing the scaled value by the scaling factor, C. The scaled shielding anisotropies, $\Delta\sigma'$, and refined principal components of the two inequivalent shielding tensors of $3CdSO_4 \cdot 8H_2O$ are listed in Table I.

Values of the shielding components, σ_i, generated by the OMAS experiments were used as initial guesses in a nonlinear, least-squares synthesis[8] of the static spectrum of $3CdSO_4 \cdot 8H_2O$. The powder patterns of the shielding tensors, thus obtained, are shown directly below the static spectrum in Figures 1 and 2. Mean values of the shielding components in ppm compiled from static, OMAS, and MAS data (one standard deviation in parentheses) are: $\sigma_\parallel^A = -99.6$ (4.2), $\sigma_\perp^A = -15.6$ (1.9), $\bar{\sigma}^A = -43.6$ (0.1), $\Delta\sigma^A = -84.0$ (6.2); $\sigma_\parallel^B = -127.4$ (2.4), $\sigma_\perp^B = -21.0$ (0.8), $\bar{\sigma}^B = -56.4$ (0.3), $\Delta\sigma^B = -106.3$ (3.2). A discussion of the ^{113}Cd shielding parameters in the salt $Cd(NO_3)_2 \cdot 4H_2O$ and their similarities/differences with those in $3CdSO_4 \cdot 8H_2O$ follows.

Solid-state ^{113}Cd studies[2] of the salt $Cd(NO_3)_2 \cdot 4H_2O$ show only one type of Cd(II). Its shielding tensor is axially symmetric and the shielding parameters are: $\sigma_\parallel = -126$, $\sigma_\perp = 63$, $\Delta\bar{\sigma} = -189$, and $\bar{\sigma} = 0$ ppm. Crystallographic[9] measurements of $Cd(NO_3)_2 \cdot 4H_2O$ show orthorhombic crystals and only one type of Cd(II) coordinated with eight oxygens located at the eight vertices of a distorted polyhedron. Four of the encapsulating oxygens are from water (Cd–O distances of 2.26 and 2.33 Å) and four are from the nitrate (Cd–O distances of 2.44 and 2.59 Å). Cadmium(II) lies at the center of this polyhedron on a twofold axis.[9] An illustration of this oxygen coordination sphere which shows the locations of oxygens from the water and nitrate is shown in Figure 3.

The occurrence of the symmetry axis suggests a possible orientation of the shielding tensor: shielding associated with the unique component, $\sigma_\parallel$, is in the direction of the twofold axis and equivalent shieldings associated with the degenerated components, $\sigma_\perp$, are in directions perpendicular to this axis. Since the observed

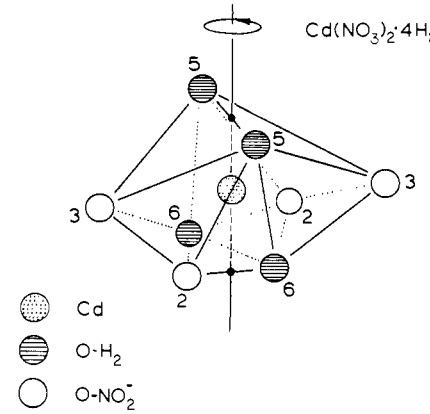

Figure 3. An illustration of the cadmium–oxygen environment in the salt $Cd(NO_3)_2 \cdot 4H_2O$.

shielding anisotropies of $3CdSO_4 \cdot 8H_2O$ are also axially symmetric, within experimental error of 4 ppm, we would expect a fairly symmetric arrangement of oxygens about each inequivalent cadmium. In fact, the special sites in the monoclinic unit cell of $3CdSO_4 \cdot 8H_2O$, discussed below, do have twofold symmetry.

One might expect O-coordination from water and nitrate groups to show selective influences on different shielding components, although which of the two shielding components, $\sigma_\parallel$ and $\sigma_\perp$, is more affected by O-coordination from water or nitrate is somewhat uncertain. There is some evidence that O-coordination from water affects $\sigma_\parallel$. It should be particularly noted that $\sigma_\parallel$ of type B Cd(II) in $3CdSO_4 \cdot 8H_2O$ and $\sigma_\parallel$ of Cd(II) in $Cd(NO_3)_2 \cdot 4H_2O$ are approximately equal. Also, $\sigma_\parallel$ of type A Cd(II) has a similar value. Since both compounds contain water, one may speculate that the $\sigma_\parallel$ component is directly affected by O-coordination with water. Therefore, the Cd(II)–O(water) bonding distance might be expected to be similar in both salts.

Isotropic shielding values, $\bar{\sigma}$, correspond to the average shielding at a given nucleus. While type B Cd(II) is slightly deshielded from type A Cd(II) in $3CdSO_4 \cdot 8H_2O$, they are both noticeably downfield from the Cd(II) in $Cd(NO_3)_2 \cdot 4H_2O$. The observed deshielding of both Cd(II) in $3CdSO_4 \cdot 8H_2O$ relative to that in the nitrate is consistent with Lipson's crystal structure, which has each Cd(II) site surrounded by six nearest neighbor oxygens as compared with eight oxygens for the Cd(II) in $Cd(NO_3)_2 \cdot 4H_2O$. Integrated NMR intensities are well within experimental error of the 2/1 ratio based on the ratio of general to special sites in the unit cell of Lipson's crystal structure.[3]

Shielding anisotropies, $\Delta\sigma$, are characteristic of the three-dimensional shielding environment and thus can serve as a useful probe of the variation in O-bonding distances. Since the observed anisotropies of Cd(II) in $3CdSO_4 \cdot 8H_2O$ are roughly half the anisotropy of Cd(II) in $Cd(NO_3)_2 \cdot 4H_2O$, one might expect a narrower range of oxygen bonding distances in 3 $CdSO_4 \cdot 8H_2O$ compared to those found[9] in $Cd(NO_3)_2 \cdot 4H_2O$ which vary from 2.26 to 2.59 Å. Clearly, the wider range in O-bonding distances proposed by Lipson (2.12 to 2.63 Å) would seem to be incompatible with the smaller anisotropies of the ^{113}Cd shielding tensors in $3CdSO_4 \cdot 8H_2O$.

Because of the possibility of a lack of precision in the Cd–O bonding distances in Lipson's original crystal structure,[3] Richardson and Jacobsen[10] have reinvestigated the crystal structure of $3CdSO_4 \cdot 8H_2O$. Their refined crystal structure is similar to Lipson's original structure: the unit cell is monoclinic with virtually identical structural parameters and has four $3CdSO_4 \cdot 8H_2O$ per unit cell and two inequivalent sites which are referred to as general "g" and special "s" positions. Special positions contain a twofold axis and there are two general positions for each special position. However, the Cd–O bonding distances are much more uniform than those in Lipson's original structure. All subsequent dis-

(8) Murphy, P. D.; Gerstein, B. C. "Analyses and Computerized Fitting of the Lineshape of the NMR Powder Pattern", DOE Report IS-4516 (revised), unpublished.

(9) Matkovic, B.; Ribov, B.; Zelenko, B.; Peterson, S. W. *Acta Crystallogr.* **1966**, *21*, 719.

(10) Richardson, J. W.; Jacobsen, R. A. *Cryst. Struct. Comm.*, submitted for publication.

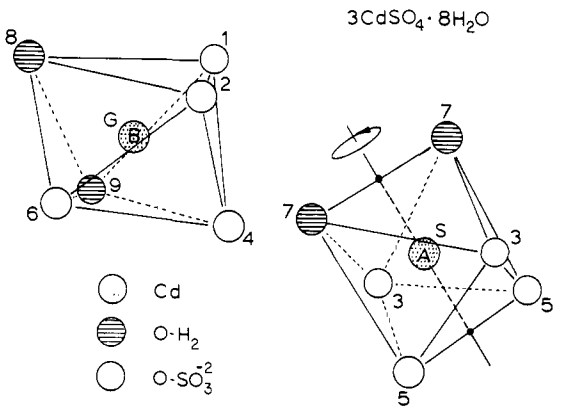

Figure 4. An illustration of the cadmium–oxygen environment for the two inequivalent cadmium sites in the salt $3CdSO_4 \cdot 8H_2O$.

cussions are based on Richardson and Jacobsen's refined crystal structure of $3CdSO_4 \cdot 8H_2O$.[10]

The high-resolution ^{113}Cd NMR spectra of this compound which are shown in Figures 1 and 2 display two magnetically inequivalent resonances labeled "A" and "B". The average percent areas obtained from static, MAS and OMAS experiments, with one standard deviation in parentheses, are: 33.8 (1.3)%, type A; and 66.2 (1.2)%, type B. These areas are well within experimental error of the expected 2/1 ratio.

The more deshielded absorption "B" is thus assigned to Cd(II) located at the general positions and the more shielded absorption "A", to Cd(II) located at the special positions. The cadmium atoms at both positions are each coordinated with six nearest neighbor oxygens: four from sulfate and two from water. An illustration of the Cd–O environments at each of the two sites is shown in Figure 4. The special sites have identical Cd–O(sulfate) bonding distances of 2.31 Å for the two inequivalent sulfate oxygens and Cd–O(water) bonding distances of 2.30 Å. The general sites have Cd–O(sulfate) bonding distances which range from 2.23 to 2.33 Å and Cd–O(water) bonding distances of 2.29 and 2.30 Å.

Nolle[11] has measured the ^{113}Cd shieldings of the cadmium chalcogenides. His shieldings are reported with respect to an atomic reference scale. We have measured the isotropic shifts (first moments) and linewidths (full widths at half-maxima in parentheses) of ^{113}Cd in CdS and CdO as: −808 ± 5 (9) and −515 ± 15 (176) ppm, respectively. Isotropic shifts are referenced to the ^{113}Cd in $Cd(NO_3)_2 \cdot 4H_2O$. As was reported by Nolle,[11] we have also encountered an unusually large linewidth for the oxide which is ca. 2.2 kHz at our Larmor frequency. We have used the isotropic shift of the ^{113}Cd of the CdS (which we believe to be the more accurate of the two samples owing to the large line linewidth of the oxide) to correlate shieldings on our nitrate scale to those on Nolle's atomic reference scale. Shielding, σ_N, referenced to $Cd(NO_3)_2 \cdot 4H_2O$ may be converted to shielding, σ_A, on Nolle's atomic reference scale with the following equation:

$$\sigma_A = \sigma_N - 984 \text{ ppm} \quad (9)$$

Using the above relationship, one finds that Nolle's isotropic shift of the ^{113}Cd in CdO occurs at −535 ppm with respect to $Cd(NO_3)_2 \cdot 4H_2O$. The Cd(II) in CdO have octahedral coordination with six nearest-neighbor oxygens (NaCl structure). The Cd–O bonding distance is 2.35 Å.

Both the static and MAS ^{113}Cd spectra of $CdSO_4 \cdot H_2O$ are shown in Figure 5, and appropriate spectral information is tabulated in Table II. The powder $CdSO_4 \cdot H_2O$ contains a single ^{113}Cd species whose isotropic shift lies close to type A Cd(II) of $3CdSO_4 \cdot 8H_2O$. However, and most remarkably, the shielding tensor is nonaxially symmetric with an anisotropy from 30 to 50 ppm larger than either of the axially symmetric tensors observed in $3CdSO_4 \cdot 8H_2O$, and the proton spin–lattice relaxation time, T_1, is ca. three times longer than that in $3CdSO_4 \cdot 8H_2O$. As far as

(11) Nolle, A. *Z. Naturforsch. A* **1978**, *33*, 666.

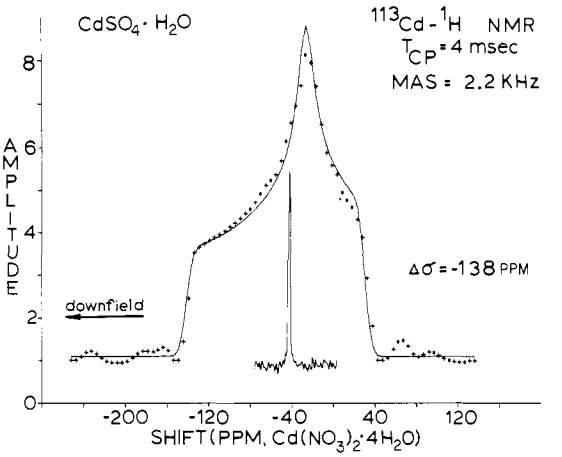

Figure 5. Solid-state spectrum of ^{113}Cd of $CdSO_4 \cdot H_2O$ showing a nonaxially symmetric shielding tensor. Also shown is the MAS-narrowed spectrum.

Table II. ^{113}Cd Shielding Parameters for $CdSO_4 \cdot H_2O$

conditions	σ_{11}[a] ± 5 ppm	σ_{22} ± 5 ppm	σ_{33} ± 5 ppm	$\bar{\sigma}$	$\Delta\sigma$[e] ± 10 ppm	fwhm[b]	R[c] ± 20 Hz
static	−139	−31	28	−47[f]	−138	12[f]	1140
MAS				−42.4[g]		2.2[d,g]	

[a] See footnote *b* in Table I. [b] Full width at half-maximum of Gaussian broadening function. [c] Rapid rotation criterion; ω_0 = 12.42 MHz (eq 6 in text). [d] Full width at half-maximum absorption. [e] $\Delta\sigma = \sigma_{11} - (\sigma_{22} + \sigma_{33})/2$. [f] Precision ± 5 ppm. [g] Precision ± 0.5 ppm.

Table III. Comparison of Cd–O Average Bonding Distances and Bonding-Distance Anisotropies with Isotropic and Anisotropic ^{113}Cd NMR Shielding Parameters

salt	O coord no.	av distance, Cd–O, Å	$\bar{\sigma}$ ± 5 ppm[a]	anisotropy Cd–O distance, Å	$\lvert\Delta\sigma\rvert$, ppm[b]
$Cd(NO_3)_2 \cdot 4H_2O$	8	2.41	0.0	0.33	189
$3CdSO_4 \cdot 8H_2O$ "g" site	6	2.28	−56.4	0.10	106
$3CdSO_4 \cdot 8H_2O$ "s" site	6	2.31	−43.6	0.01	84
CdO	6	2.35	−515[d]	0.0	0.0[c]

[a] Isotropic shift in ppm with respect to $Cd(NO_3)_2 \cdot 4H_2O$. [b] Magnitude of NMR shielding anisotropy. [c] Large residual broadening may have obscured a small anisotropy. [d] Uncertainty ±15 ppm.

we know, the X-ray crystal structure of $CdSO_4 \cdot H_2O$ has never been reported.

A comparison of average Cd–O bonding distances and bonding-distance anisotropies (i.e., absolute differences between maximum and minimum distances) with NMR isotropic shieldings, $\bar{\sigma}$, and anisotropies, $\Delta\sigma$, is presented in Table III. A strong correlation appears to exist between bonding-distance anisotropies and NMR shielding anisotropies. In general as the *range* of nearest-neighbor oxygen bonding distances increases at a particular Cd(II) site, the observed shielding anisotropy also increases. For instance, because the Cd(II) site in $CdSO_4 \cdot H_2O$ has a larger anisotropy than either Cd(II) site in $3CdSO_4 \cdot 8H_2O$, one might expect less uniformity in Cd–O bonding distances in the former.

Correlations of average Cd–O bonding distances with isotropic shifts are not obvious. For example, the "s" site of $3CdSO_4 \cdot 8H_2O$ has a larger average Cd–O bonding distance than the "g" site. We might expect the ^{113}Cd site, at which the average Cd–O bonding distance is larger, to be the more deshielded. However, the exact opposite is actually observed.

In summary, the principal components of the ^{113}Cd shielding tensors of hydrated cadmium sulfate salts are shown to be particularly sensitive to the coordination of Cd(II) with oxygen. NMR shielding anisotropies are shown to reflect the variations

of Cd-O bonding distances. Prompted by an anomaly between the observed shielding anisotropies of the magnetically inequivalent ^{113}Cd in $3CdSO_4 \cdot 8H_2O$ and the proposed Cd-O bonding distances, a refinement[10] of the X-ray crystal structure of this salt has shown a much more uniform distribution of Cd-O bonding distances than was originally[3] proposed.

Acknowledgment. The authors thank (1) Dr. H. F. Franzen and Robert Kematick for the Guinier X-ray powder measurements and other discussions; (2) Gary Austin and Robert Hofer of the Ames Lab Analytical Services for the determinations of H_2O/Cd mole ratios, and (3) Gary Robbins for assistance in the use of ORTEP to draw the various crystal structures.

UPE Studies of Conjugation Involving Group 5A Elements. 1. Phenylphosphines

Diane E. Cabelli, Alan H. Cowley,* and Michael J. S. Dewar*

Contribution from the Department of Chemistry, The University of Texas at Austin, Austin, Texas 78712. *Received October 15, 1979*

Abstract: UPE spectra are reported for phenylphosphine, *p*-phenylenediphosphine, phenyldichlorophosphine, *p*-phenylenebis(dichlorophosphine), phenylbis(diethylamino)phosphine, and *p*-phenylenebis(diethylamino)diphosphine. Analysis using PMO theory indicates that the assignments in phenylphosphine and aniline are similar, I_1 in each case corresponding to ionization from a perturbed benzene π MO, I_3 to a perturbed lone pair. This conclusion agrees with the well-established assignment for aniline but differs from that previously suggested for phenylphosphine. Our conclusions are supported by MNDO calculations.

A problem which has remained of topical interest for many years concerns the extent to which trivalent elements of group 5A can undergo conjugative interactions with the π electrons of adjacent conjugated systems via their lone pair electrons. The existence of such interactions has long been recognized in the case of nitrogen, as, for example, between nitrogen and the benzene ring in aniline (**1**). Here the interaction leads to changes in chemical behavior, as exemplified by the low basicity of **1**. Effects of this kind are, however, likely to be smaller in the case of other group 5A elements, in particular phosphorus.

The development of ultraviolet photoelectron (UPE) spectroscopy has provided a valuable tool for studying conjugative interactions in molecules,[1] on the basis of interpretation of UPE spectra in terms of MO theory and Koopmans' theorem.[2] Studies of this kind have established the existence of strong conjugative interactions in unsaturated amines such as **1**[3] and also in phenylphosphine (**2**).[4] Some confusion seems to have been caused here by failure to distinguish between collective and one-electron properties of molecules.[5] It is quite possible for conjugative interactions to lead to large changes in the energies of individual MOs (and hence in one-electron properties associated with those MOs) without significantly affecting the total energy of the molecule (and hence its collective properties). The UPE data for **1** and **2** therefore give no indication of the extent to which the observed conjugative interactions will affect their chemical reactivity and other collective properties. Nevertheless the orbital interactions are clearly of interest in their own right.

Analysis of the UPE spectrum of **2**, using the PMO[6] approach first applied to benzene derivatives by Turner et al.,[7] indicates the existence of a strong conjugative interaction between phosphorus and the ring. The HOMO of benzene consists of a pair of degenerate π MOs which, in real form and C_{2v} symmetry, are indicated in Figure 1. We will follow the usual convention of continuing to use the C_{2v} description (a_2,b_1), even in cases when substitution destroys the C_{2v} symmetry. In **2**, with phosphorus attached to C_1 of benzene (Figure 1), the phosphorus lone pair AO(p) does not interact with the a_2 MO. The ionization corresponding to this should remain virtually unchanged in the UPE spectrum of **2**. Indeed, I_2 for **2** (9.37 eV) is similar to that for benzene (9.24 eV). The small difference can be attributed to miscellaneous second-order effects (inductive effect, field effect, interactions with phosphorus 3d AOs and/or the PH bonds, which, in **2**, do not lie in the nodal plane of the ring). I_1 and I_3 then correspond to the p and b_1 orbitals. The fact that b_1 is considerably

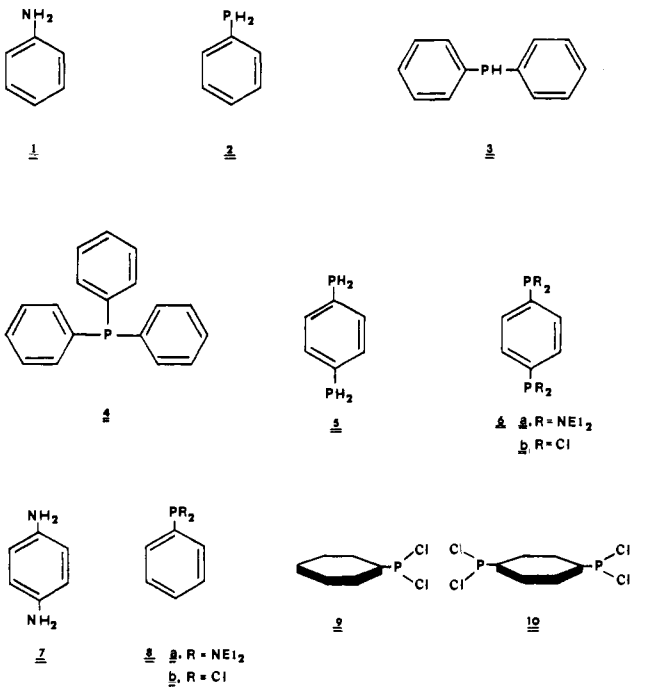

(1) See: (a) Turner, D. W.; Baker, A. D.; Baker, C.; Brundle, C. R. "*Molecular Photoelectron Spectroscopy*"; Wiley: New York, 1970. (b) Bock, H.; Ramsey, B. G. *Angew Chem., Int. Ed. Engl.* **1973**, *12*, 734. (c) Rabalais, J. W. "*Principles of Ultraviolet Photoelectron Spectroscopy*"; Wiley: New York, 1977.

(2) Broglie, F.; Clark, P. A.; Heilbronner, E.; Neuenschwander, M. *Angew Chem., Int. Ed. Engl.* **1973**, *12*, 422.

(3) Maier, J. P.; Turner, D. W. *J. Chem. Soc., Faraday Trans. 2* **1977**, 69, 521.

(4) Debies, T. P.; Rabalais, D. W. *Inorg. Chem.* **1974**, *13*, 308.

(5) See: Dewar, M. J. S. *Chem. Eng. News* **1965**, *43*, 86. "The Molecular Orbital Theory of Organic Chemistry"; McGraw-Hill: New York, 1969.

(6) Dewar, M. J. S. *J. Am. Chem. Soc.* **1952**, *74*, 3341, 3345, 3350, 3353, 3355, 3357. Dewar, M. J. S.; Dougherty, R. C. "The PMO Theory of Organic Chemistry"; Plenum: New York, 1975.

(7) Turner, D. W.; May, D. P. *J. Chem. Phys.* **1966**, *45*, 471; **1967**, *46*, 1156.

0002-7863/81/1503-3286$01.25/0